1 Vorticity smoothing

The time evolution in the relative vorticity is discontinuous, which is represented in the time evolution of its maximum (Fig. S1). For further analysis, it is necessary to apply a filter in order to calculate the vorticity tendency and growth rate, where we chose the Savitzky-Golay filter (Savitzky and Golay, 1964).

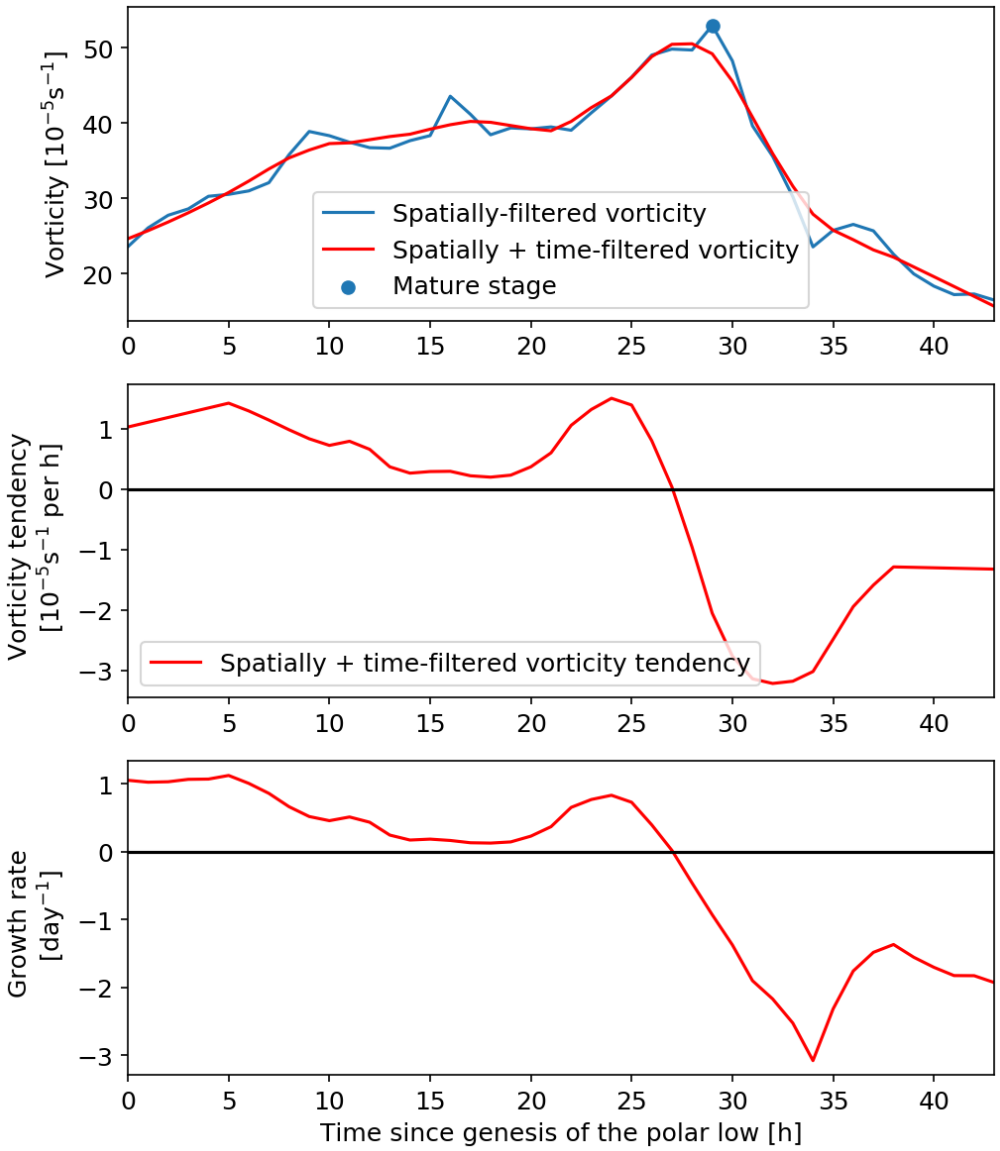

Figure S1: Demonstration of the relative-vorticity smoothing with the Savitzky-Golay filter, which is applied for the calculation of the vorticity tendency and the growth rate.

2 Different SOM matrices

The dimension of the SOM matrix has to be determined a priori. In order to demonstrate that the choice of the matrix size does not alter the results, we show the result for a 4×5 matrix in Figure S2. The result is very similar to the 3×3 matrix chosen in our study (Fig. S3). In the corners are the forward (node 1), right (node 4), reverse (node 20), and left-shear (node 17) conditions. Along the edges are intermediate situations between the corners with varying tilts. Towards the middle, the temperature gradient decreases. We consider that the 3×3 SOM matrix condenses this large SOM matrix while still containing the most relevant information.

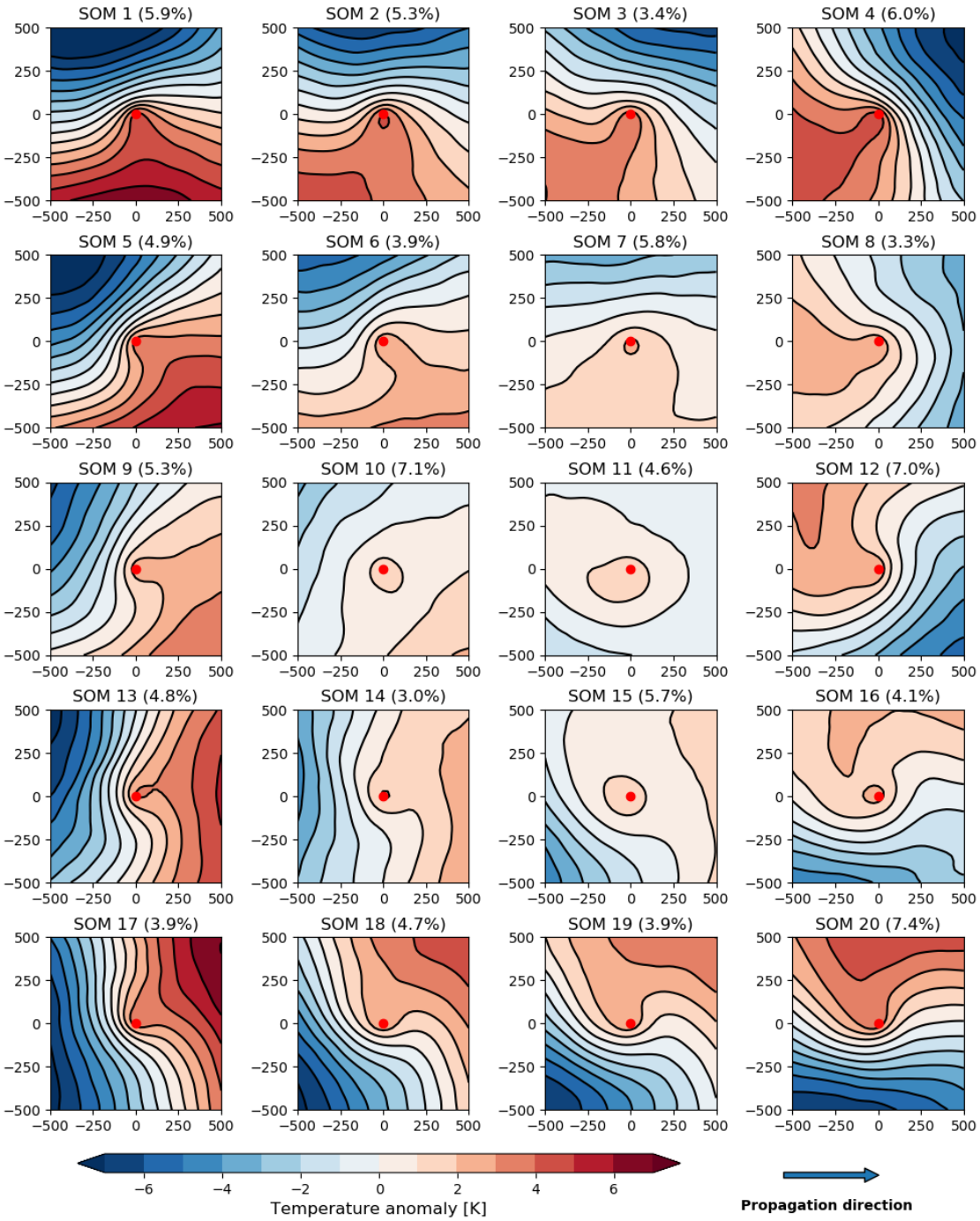

Figure S2: The SOM algorithm applied on the temperature anomaly at 850 hPa for a predefined 4×5 matrix. The fields are in a PL-centered perspective with propagation towards the right the PL located in the middle, denoted by a red dot. Presented are the composites associated to each SOM node. Contours show the same as shadings. The number in parenthesis denotes the fraction of time steps included in the respective SOM node.

3 Self-organizing maps applied to different fields

Multiple meteorological fields were tested for their application in the SOM algorithm. Generally, the SOM method is powerful in revealing patterns of variability included in the applied field.

3.1 Reasoning for the application to anomaly fields

Variability patterns are most clearly distilled when the algorithm is applied to the anomaly field (Fig. S3, S4). Figure S3 shows the result from the temperature anomaly field as used in our study. For calculation of the temperature anomaly, the mean temperature within the PL-centered grid of each individual time step is removed. In this way, the information concerning a PL time step occurring in a warm or cold environment is removed. Otherwise, the area-mean temperature dominates the SOM analysis, as can be seen in Figure S4, which shows the SOM matrix that results from application on the temperature field at 850 hPa. The nodes 7 - 9 all display reverse-shear conditions with a different mean temperature. Nodes 1, 2 and 4 represent forward-shear environments with a different background temperature. Node 6 and 3 feature left and weak-shear conditions, respectively.
Hence, the most frequent shear situations are reproduced if the area-mean is not removed. However, the SOM matrix includes several nodes that display the same shear situations just in warmer or colder environments. It it therefore more valuable to remove the mean temperature within each PL-centred grid prior the SOM analysis, as shown in Figure S3.

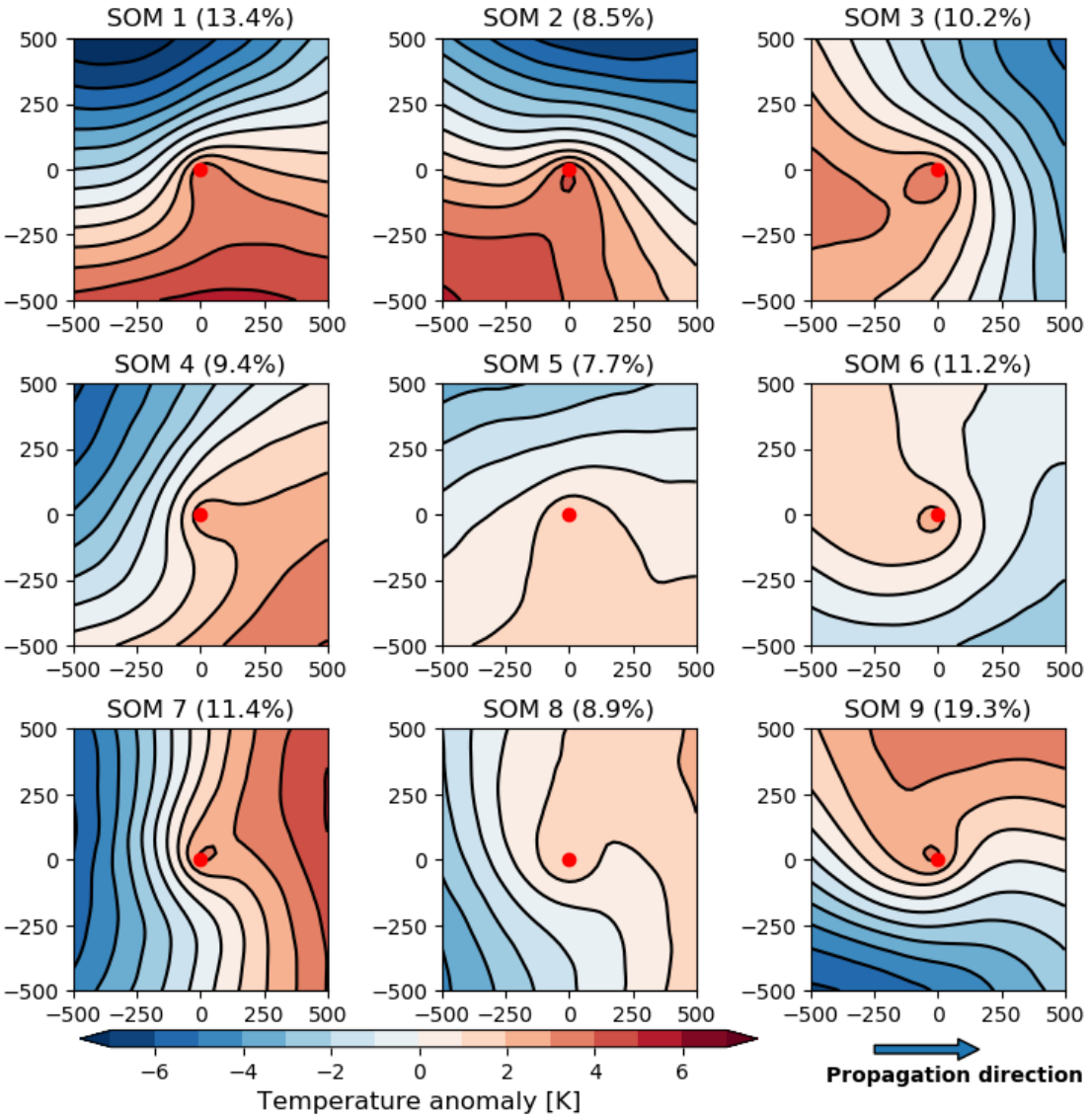

Figure S3: As Figure S2, but the SOM algorithm is applied to a predefined 3×3 matrix, as presented in Figure 2 of the paper.

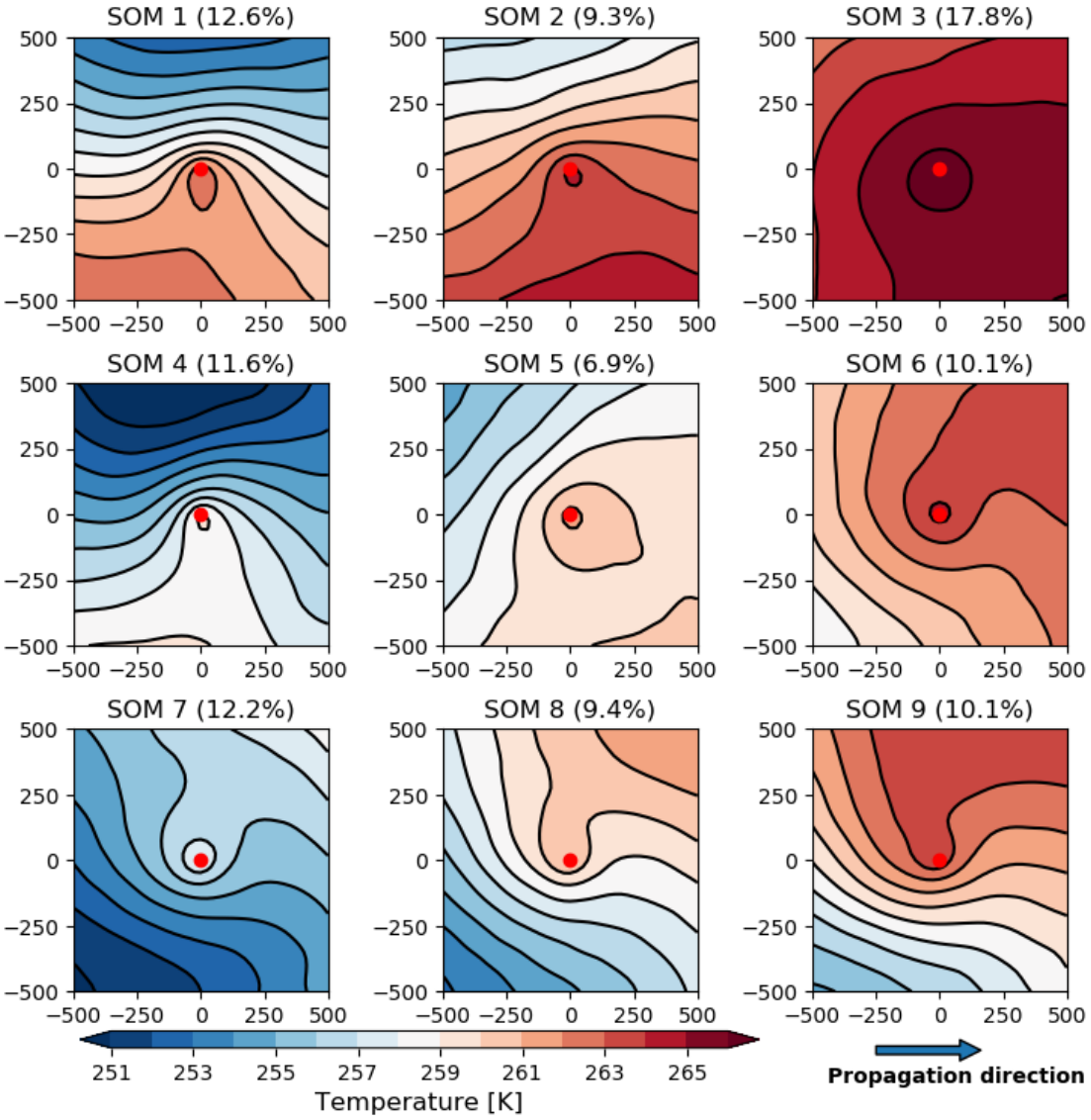

Figure S4: As Figure S3, but the SOM algorithm is applied to the temperature field at 850 hPa instead of the temperature anomaly field. Hence, the area-mean within each polar-low centered field is not removed.

3.2 Fields with similar SOM matrices to T'_{850}

The SOM algorithm captures similar patterns of variability when applied to other variables.
The SOM matrix for the temperature anomaly field at 500 hPa (Fig. S5) and 1000 hPa (not shown) looks very similar to the one at 850 hPa (Fig. S5). The same orientations of the thermal field are reproduced. Even the frequency occurrence of the nodes is in a comparable range. Different to the temperature anomaly at 850 hPa (Fig. S3), the fields at 500 hPa are less influenced by the circulation of the PL itself.
The SOM matrix in the specific humidity anomaly at 850 hPa (Fig. S6) displays similar patterns as the temperature anomaly matrix of the same level (Fig. S3). This is explained by the higher saturation vapour pressure at higher temperatures due to the Clausius-Clapeyron relation. However, in the SOM matrix of the specific humidity anomaly, PL centres protrude as moist cores.

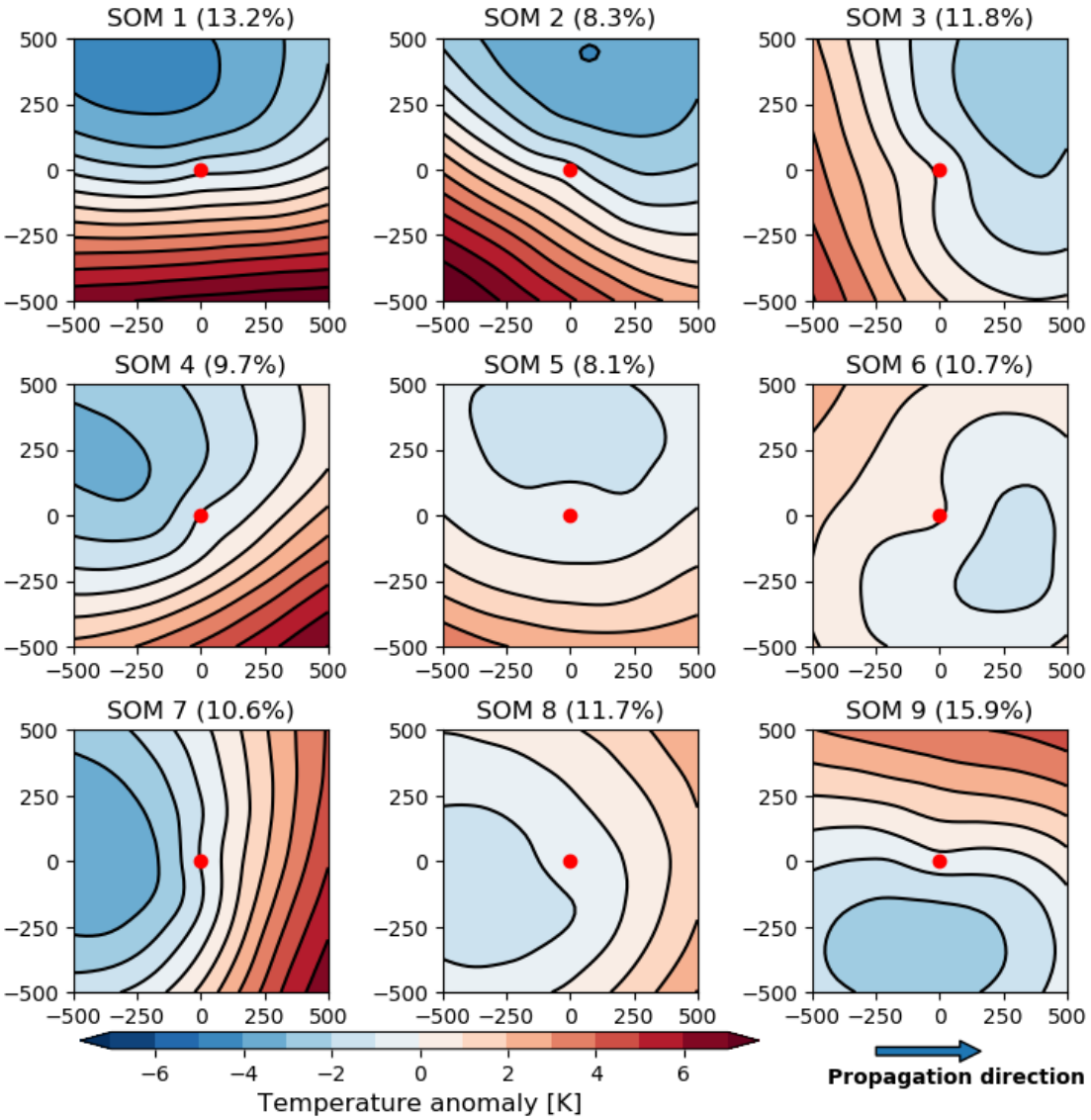

Figure S5: As Figure S3, but the SOM algorithm is applied to the temperature anomaly field at 500 hPa instead of at 850 hPa.

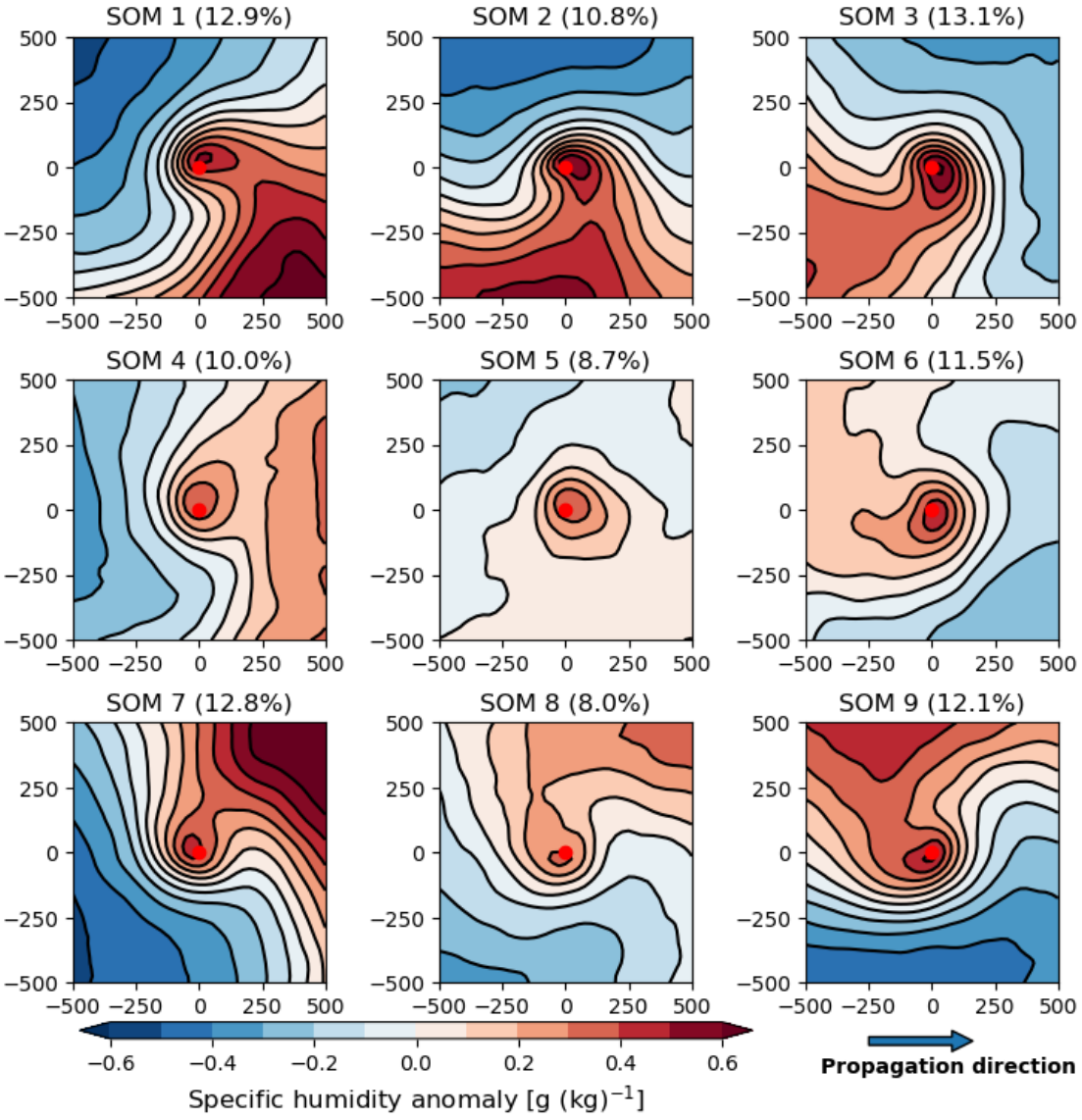

Figure S6: As Figure S3, but the SOM algorithm is applied to the specific humidity anomaly field at 850 hPa instead of the temperature anomaly field.

3.3 Fields with SOM matrices displaying little variability

Different from the other presented fields, the nodes are quite similar to each other within the SOM matrix for the geopotential height anomaly at mid-levels (700 hPa, Fig. S7). Similar SOM nodes can be associated to a rather small variability in the field. PLs are generally associated with a trough of a synoptic-scale low pressure system on the left-hand side of the PL with respect to its propagation direction. The low pressure is associated with a synoptic-scale background flow. The variability among PLs, expressed by the different SOM nodes, is organised along different strengths of the background flow (strong in the first column of the matrix and weak in the last one) as well as a different tilt of the trough axis (slightly to the top-right in the first row of the matrix, symmetric in the middle row, and to the top-left in the bottom row). The small variability in the mid-level flow around the PLs can be explained by the mid-level flow largely determining the propagation direction of the PLs. The PL-centred perspective rotated in propagation direction captures the mid-level flow variability to a large degree.

Also the relative vorticity field at 850 hPa PLs shows only small variability, as the SOM nodes are quite similar (Figure S8) [1]. All nodes reproduce an area of high vorticity for the PL centre and negligible vorticity in the environment. Some nodes display a circular and others a more elliptical vorticity field, where the orientation of the ellipse varies. Also the strength in the vorticity maxima is different among the nodes.

The results from the mid-level geopotential height anomaly and the relative vorticity suggests that PLs can be considered as secondary, almost axis-symmetric vortexes embedded in a synoptic-scale flow that is oriented approximately in the direction of propagation. The superposition of the synoptic-scale flow and the PL vortex results generally in a mid-level trough.

Since the environmental flow at mid-levels is approximately parallel to the propagation direction of the PL, the circulation associated with the PL intensifies (weakens) the flow on the right (left)-hand side of the PL centre with regard to the propagation direction. Hence, the location of the strongest horizontal winds at mid-levels is mainly determined by the propagation direction of the PL, and located on the right side with regard to the propagation direction (Fig. S7).

For the same reason the strongest near-surface winds are predominantly found on the right side of the PL track (Paper Figure 8 g, i), however the environmental background flow at low levels has different strength and orientations for the different shear categories. The low-level background flow is strong for reverse shear systems, which leads by superposition to high near-surface winds (Paper Figure 5f) to the right of the propagation direction (Paper Figure 8 a, c). In forward-shear situations the low-level background flow is weak, leading to a dominance of the PL vortex at low levels, whereby the location of the wind maxima is less prominent and maximum near-surface wind speeds often somewhat lower than for the other shear categories (Paper Figure 5f). For right (left) shear situations the low-level background flow is towards the front left (right) and hence the strongest winds are located in the sector between (against) the propagation direction and its right (Paper Figure 8 d, j).

[1] For the relative vorticity the anomaly is not required, since the variable is centred around 0.

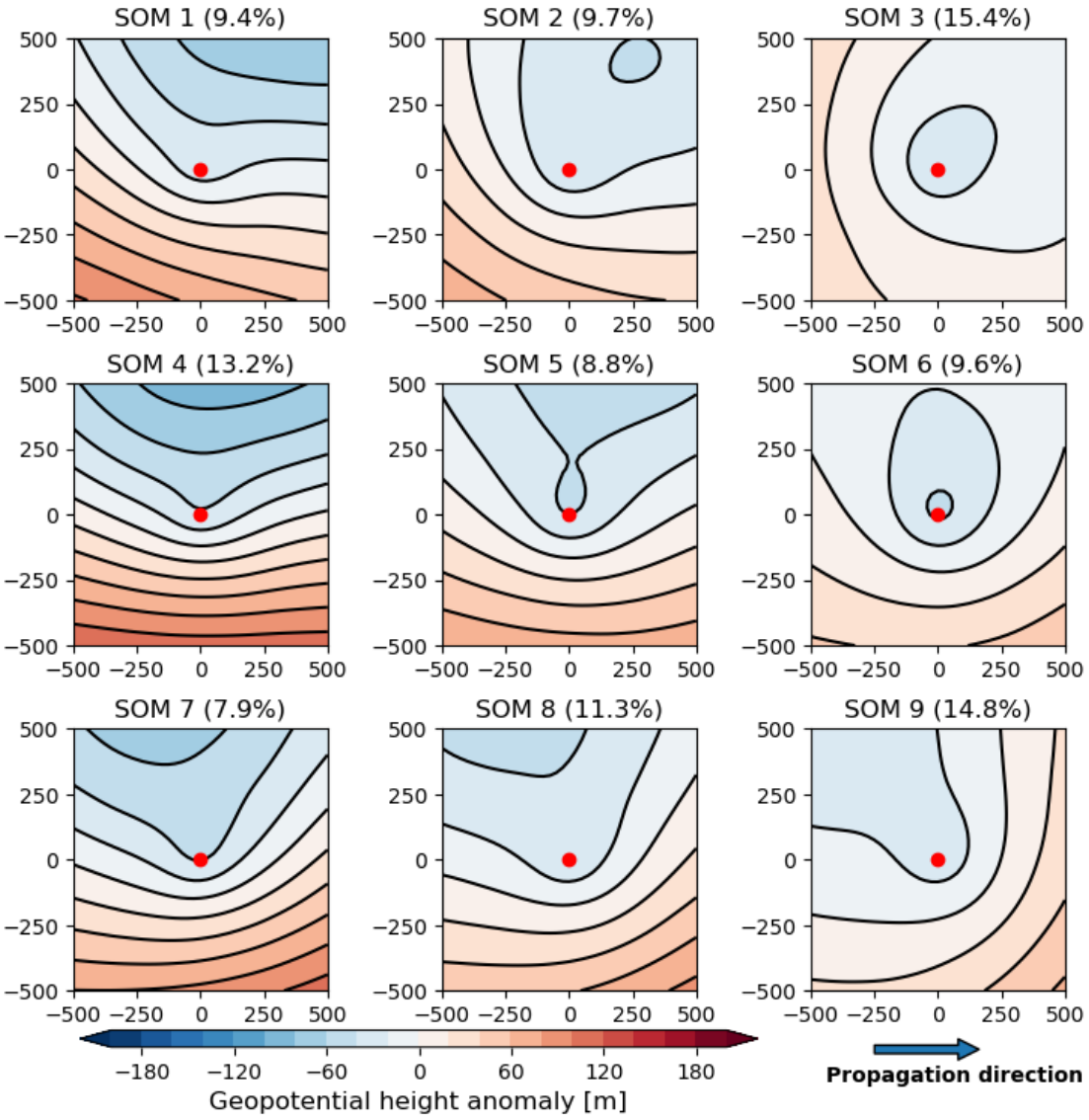

Figure S7: As Figure S3, but the SOM algorithm is applied to the geopotential height anomaly field at 700 hPa.

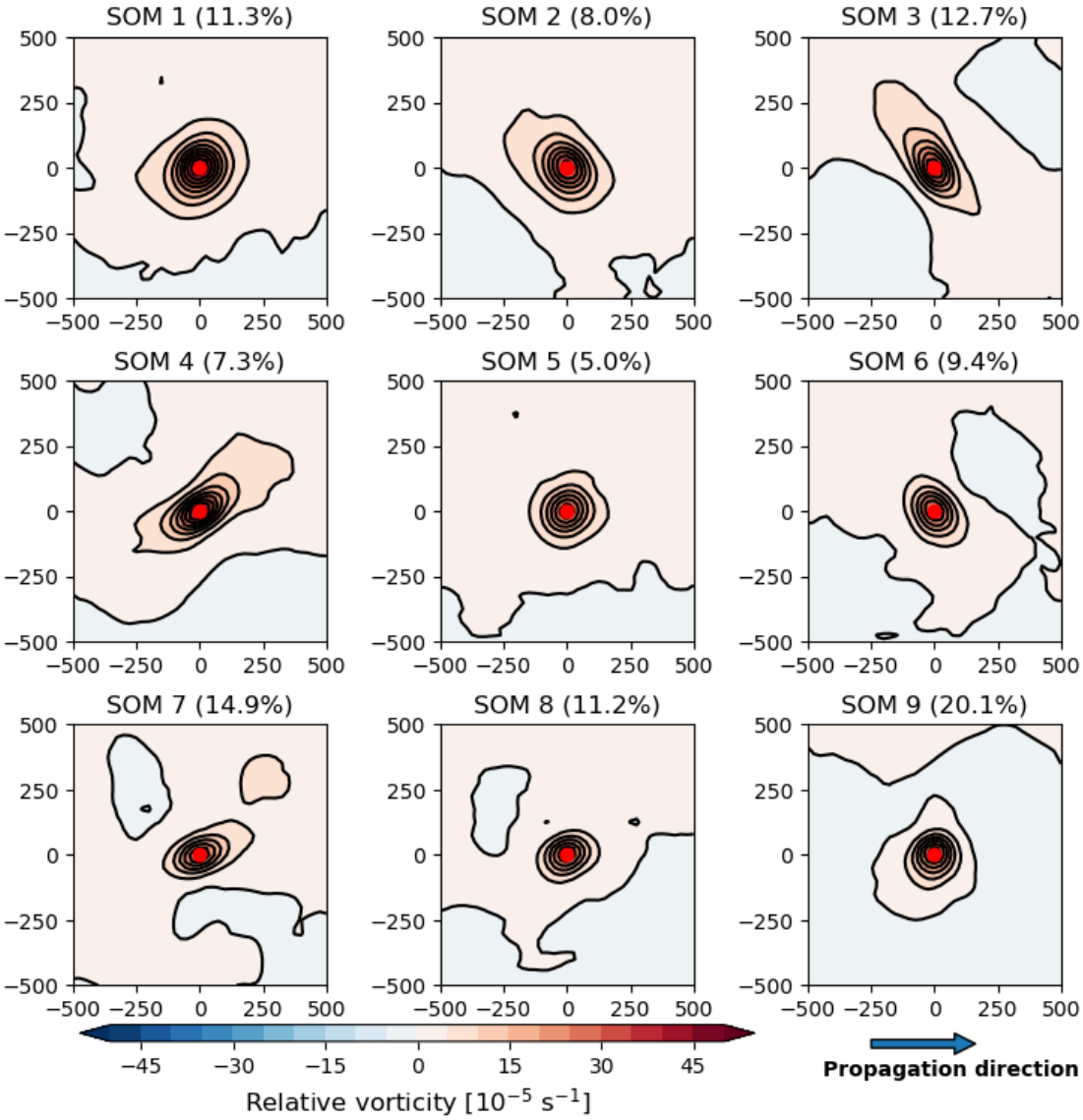

Figure S8: As Figure S3, but the SOM algorithm is applied to the relative vorticity field at 850 hPa.

3.4 Fields with equivalent SOM matrices to T'_{850}.

The SOM algorithm applied to the geopotential height anomaly at 1000 hPa (Fig. S9) produces a node with an almost closed circulation (node 1), which is typical for forward-shear PLs (see black contours in Fig. 2 of the paper). It produces a node with a strong low-level trough (node 9), which is observed for revers-shear PLs. Further a node with a trough tilted to the right (node 3) and left (node 7) are reproduced, which are typical for right and left-shear situations, respectively. Hence, the patterns produced by the application of the SOM algorithm to the low-level geopotential height field are similar to the composites in this field of the SOM nodes produced by the temperature anomaly field at 850 hPa. Similarly the SOM algorithm applied to the upper-level geopotential height anomaly (500 hPa, Fig. S10) reproduces the same patterns as the corresponding composites for the SOM nodes using the temperature anomaly field at 850 hPa (see green contours in Fig. 2 of the paper).

The equivalence of the SOM matrices from upper and lower-level flow fields to the temperature anomaly field can be explained: The geopotential height fields at mid-levels (700 hPa) are quite similar in the environment of PLs (previous section), and a horizontal temperature gradient field is connected to a vertical wind shear by the thermal wind relation, which connects the typical lower and upper-level flow patterns to the temperature anomaly pattern (Fig. S3).

We conclude that large parts of the environmental variability around PLs can be captured by the horizontal fields in only one variable. We chose to present the SOM matrix based on the temperature anomaly field at 850 hPa (Fig. S3), but the SOM matrix based on a different pressure level, the specific humidity, and the lower and upper-level geopotential height reveals qualitatively similar results.

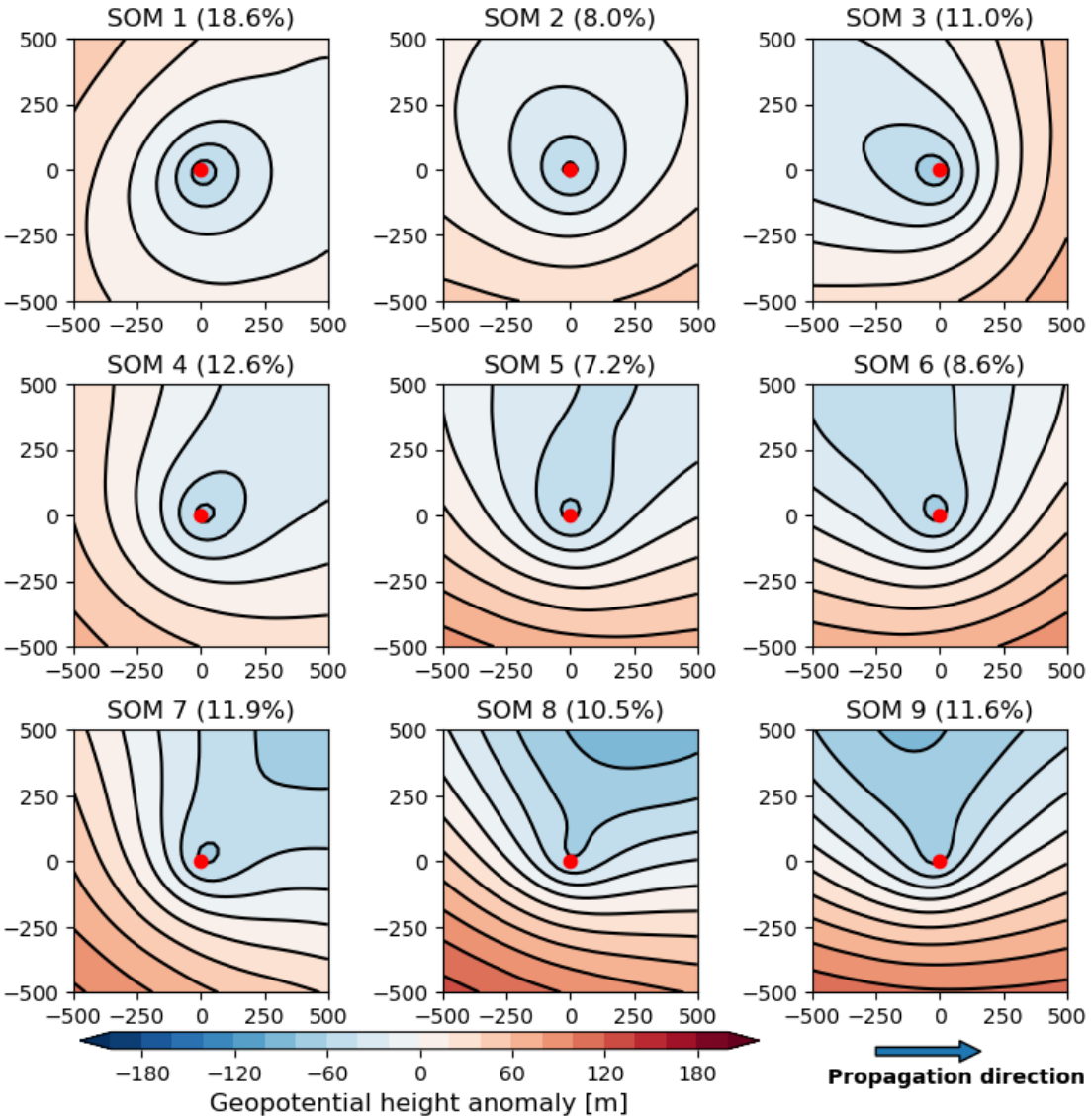

Figure S9: As Figure S3, but the SOM algorithm is applied to the geopotential height anomaly field at 1000 hPa.

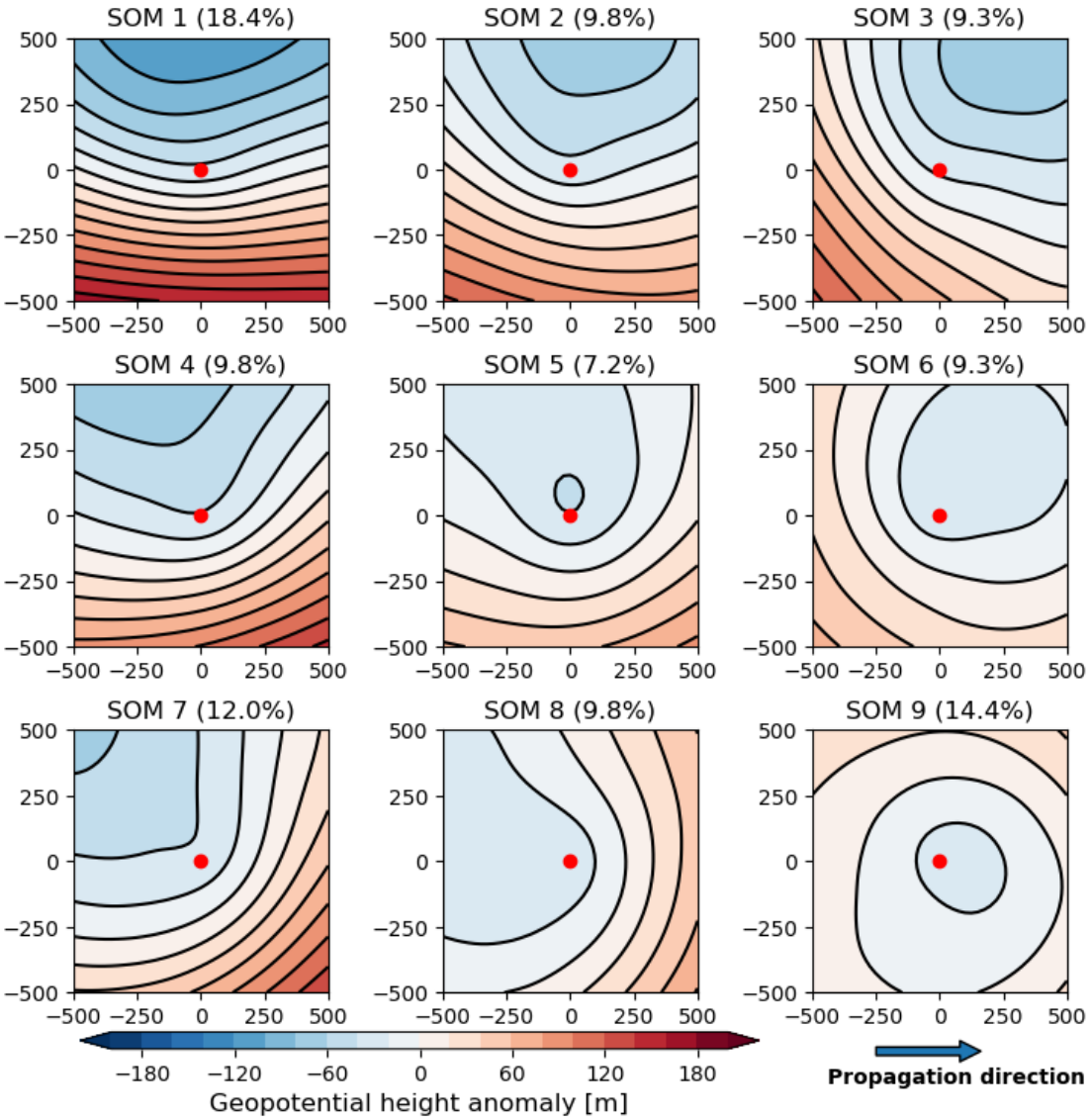

Figure S10: As Figure S3, but the SOM algorithm is applied to the geopotential height anomaly field at 500 hPa.

4 Other characteristic fields for the shear configurations

For the categories with strong vertical shear the updrafts (downdrafts) occur in the region of upper-level divergence (convergence), which is characteristic for a baroclinic organisation (Fig. S11). The vertical stability, expressed by the difference in the equivalent potential temperature between the 2 m and 500 hPa, is low (less then 6 K) around the centre of the PL, indicating almost conditional instable environments through the entire depth of the troposphere.

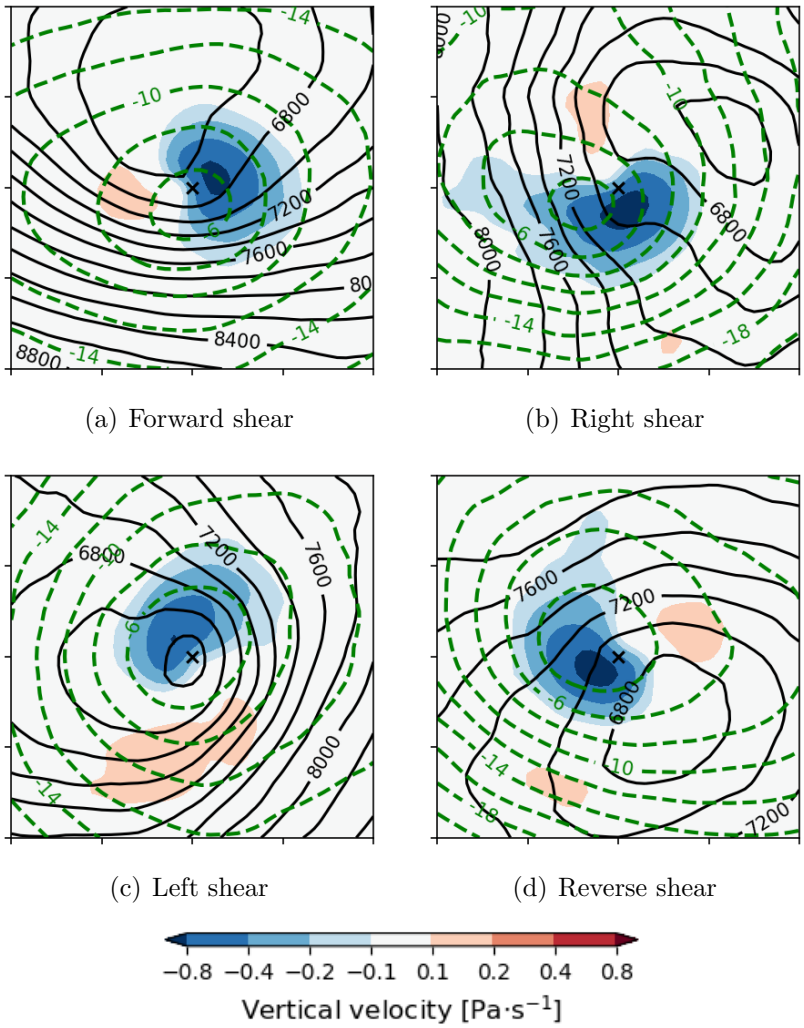

(a) Forward shear

(b) Right shear

(c) Left shear

(d) Reverse shear

Figure S11: As Figure 8 from the paper, but with the vertical velocity (shading, blue colors indicate ascent), tropopause height (black contours, 200 m spacing), and difference in the equivalent potential temperature between the 2 m and 500 hPa level (green, dashed contours, 2 K spacing).

5 Evidence for the SOM method to detect characteristic PL environments

Here, we provide more evidence that the applied SOM method is appropriate in detecting characteristic PL environments, whereas simple composites are not sufficient.

The composite fields of meteorological variables in the PL environment may fail to represent a typical PL environment. For example, the composite of all PL time steps in the 850 hPa temperature anomaly features an almost axisymmetrical thermal structure with a warm core (Fig. S12a). However, the variability in the temperature anomaly field is large (Fig. S12b), especially at some distance from the PL centre. The variability exceeds the magnitude of the composite field, which indicates that PL environments may have a considerably different structure than expressed by the composite of all time steps.

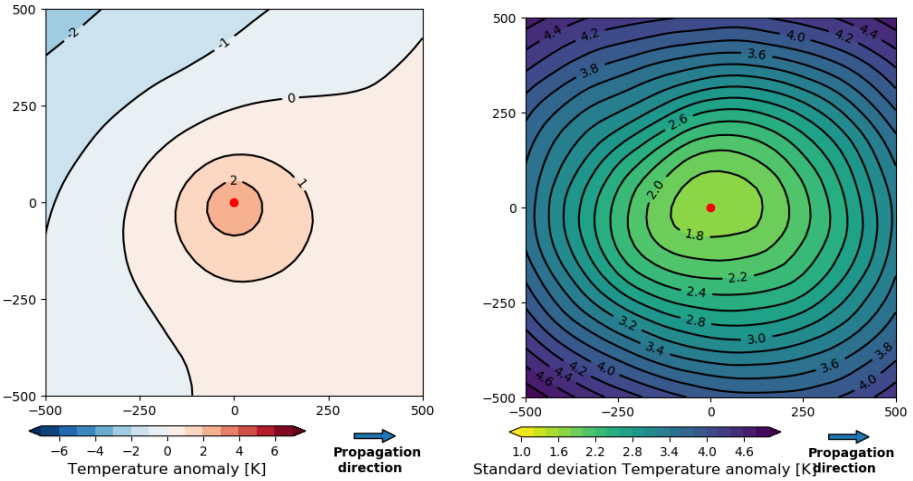

(a) Mean (b) Standard deviation

Figure S12: Mean and standard deviation in the 850 hPa temperature anomaly field in a PL centred perspective with propagation direction towards the right based on all time steps.

The SOM algorithm is a method to detect coherent patterns of variability. The SOM matrix (e.g. Fig. 2 of paper) shows that most nodes have a different structure from the composite of all time steps. The variability in the temperature anomaly is considerably lower within each SOM node (Fig. S13) than the variability among all time steps (Fig. S12b), especially at a distance of more than 100 km from the PL centre. As the variability within each SOM node is rather small and does not exceed the magnitude of its composite field, each SOM node is considered to be representative for a typical PL environment.

In the following, we discuss why the composite of all time steps features a warm-core structure, and whether PLs can be generally considered warm-core systems. The temperature anomaly most SOM nodes is characterized by strong temperature gradients and is higher at the location of the PL centre as compared to the thermal

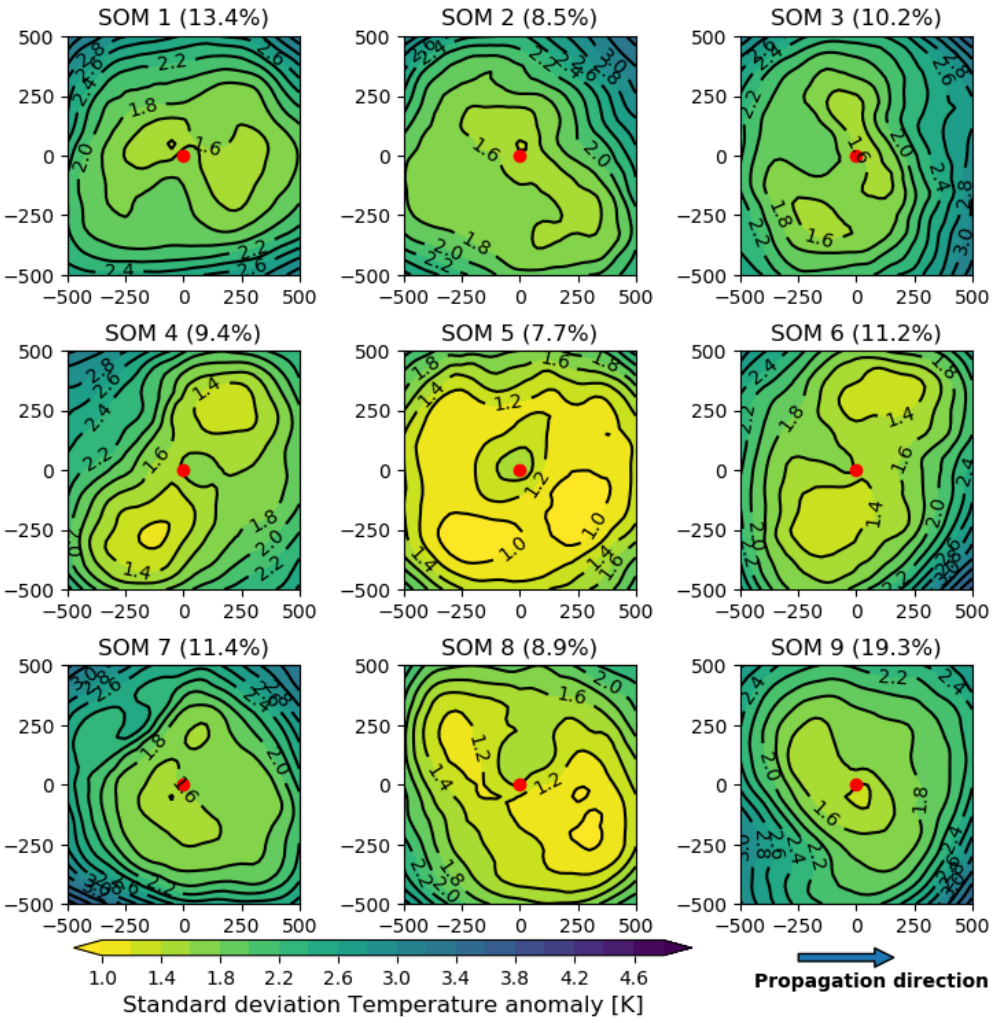

Figure S13: Standard deviation in the temperature anomaly at 850 hPa for all time steps with the same SOM node. The SOM matrix is calculated as presented in Figure 2 of the paper.

background field (e.g. Fig. 2 of the paper). It can be inferred that a mean over the thermal fields of the SOM nodes (Fig. 2 of the paper) is resulting in an axisymmetric warm-core structure captured by the composite of all time steps (Fig. S12a), whereas the thermal gradients of different orientation in the SOM nodes cancel out in the composite. The positive temperature anomaly at the centre within each SOM node could be attributed to the release of latent energy, or to the centre that is defined by the relative vorticity maximum, being located close to the updrafts in the warm conveyor belt, an area of low-level potential vorticity production. It is likely a combination the two reasons, possibly with other effects are contributing as well. Hence, PLs appear to be warm-core, but typically embedded in a background field of large thermal contrast.

The SOM algorithm also produces nodes (e.g. node 5 in Fig. 2 of the paper) with low thermal gradients, which appears like the composite of all time steps (Fig. S12a). The composite of this node features a structure that resembles an axisymmetric

warm core (more recognizable in the 4x5 SOM matrix displayed in Fig. S2). The averaging of time steps within a node might exaggerate the symmetry in the structure, by the same arguments as for the composite of all time steps. However, different from the situation with all time steps (Fig. S12), the variability is small within the symmetric SOM node (Fig. S13), which indicates that some PLs in fact have time steps with an axisymmetric warm core.
In conclusion, our method shows that axisymmetric PLs occur seldom and PL environments are instead mainly characterized by a horizontal temperature contrast.

References

Savitzky, A. and Golay, M. J.: Smoothing and differentiation of data by simplified least squares procedures., Analytical chemistry, 36, 1627–1639, 1964.